6. X. Zhuansun and X. Ma, Bilinear transform implementation of the SC-PML for general media and general FDTD schemes, IEEE Trans Electromagn Compat 54 (2012), 343–350.
7. A.A. Al-Jabr, M.A. Alsunaidi, T. Khee, and B.S. Ooi, A simple FDTD algorithm for simulating EM-wave propagation in general dispersive anisotropic material, IEEE Trans Antennas Propag 61 (2013), 1321–1326.
8. W.-J. Chen, W. Shao, and B.-Z. Wang, ADE-Laguerre-FDTD method for wave propagation in general dispersive materials, IEEE Microwave Wireless Compon Lett 23 (2013), 228–230.
9. B. Huang, G. Wang, Y.S. Jiang, and W.B. Wang, A hybrid implicit-explicit FDTD scheme with weakly conditional stability, Microwave Opt Technol Lett 39 (2003), 97–101.
10. J. Chen and J. Wang, A 3D hybrid implicit explicit FDTD scheme with weakly conditional stability, Microwave Opt Technol Lett 48 (2006), 2291–2294.
11. I. Ahmed and E.-P. Li, Convolutional perfectly matched layer for weakly conditionally stable hybrid Implicit and explicit-FDTD method, Microwave Opt Technol Lett 49 (2007), 3106–3109.
12. Z. Liu, Y. Chen, X. Sun, and Y. Liu, Implementation of CFS-PML for HIE-FDTD method, IEEE Antennas and Wireless Propag Lett 11 (2012), 381–384.
13. R. Wang and G. Wang, PLRC-WCS FDTD method for dispersive media, IEEE Microwave and Wireless Compon Lett 19 (2009), 341–343.
14. W.C. Chew and W.H. Weedon, A 3-D perfectly matched medium from modified Maxwell's equation with stretched coordinates, Microwave Opt Technol Lett 7 (1994), 599–604.
15. J.A. Roden and S.D. Gedney, Convolutional PML (CPML): An efficient FDTD implementation of the CFS-PML for arbitrary media, Microwave Opt Technol Lett 27 (2000), 334–339.

A DESIGN OF COMPACT WIDEBAND NEGATIVE GROUP DELAY NETWORK USING CROSS COUPLING

Girdhari Chaudhary and Yongchae Jeong
Division of Electronics Engineering, IT Convergence Research Center, Chonbuk National University, Jeonju, Republic of Korea; Corresponding author: ycjeong@jbnu.ac.kr

Received 16 March 2014

ABSTRACT: *This article presents a novel approach to the design of a compact wideband negative group delay (NGD) network using cross coupling between open stubs. The NGD time can be controlled by external series resistors, whereas the NGD bandwidth can be controlled by the coupling coefficient between open stubs. To verify the design concept, the NGD network operating at center frequency of 1.96 GHz was designed and fabricated. From the measurement results, a maximum achievable NGD time of −1.1 ± 0.2 ns was obtained over a 410 MHz BW with a maximum signal attenuation of 29.23 dB.* © 2014 Wiley Periodicals, Inc. Microwave Opt Technol Lett 56:2495–2497, 2014; View this article online at wileyonlinelibrary.com. DOI 10.1002/mop.28627

Key words: *cross coupling; negative group delay; wideband*

1. INTRODUCTION

In recent years, there has been an increasing amount of research on negative group delay (NGD) networks due to their interesting characteristics of time advancement in wave propagations [1–7]. The NGD, being a counterintuitive phenomenon; can be observed in certain materials as well as artificial structures within limited frequency bands under a signal attenuation (S_{21}) condition/negative refractive index [2], where it is equivalent to an increasing phase with frequency. The NGD networks have been implemented in electronic circuitry and have been applied to various practical communication systems [3–7].

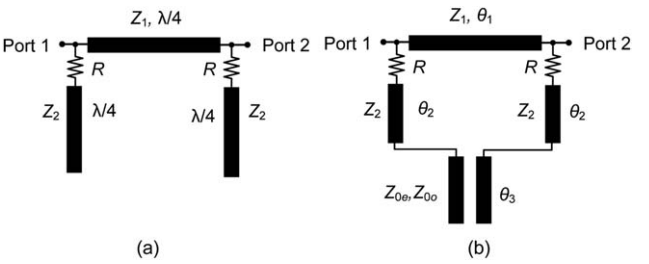

Figure 1 Structure of NGD networks: (a) conventional [6] and (b) proposed structure of wideband NGD network

Recently, a new and interesting application of the NGD network for the realization of non-Foster reactive elements, such as a negative capacitance or inductor, has been reported in [8]. It has opened a door for new application fields of NGD networks, and can also be extended to electromagnetic (EM) applications such as increasing the bandwidth of artificial magnetic conductors by loading them with NGD networks as non-Foster elements. In RF and microwaves, the series and parallel resistor-inductor-capacitor (RLC) resonators are widely used to design active/passive NGD networks [3–7, 9]. To overcome the limited availability problem of lumped elements in RF and microwave, NGD networks using distributed elements have also been presented in literature [3, 7]. However, these conventional NGD networks suffer from a narrow NGD bandwidth. Recently, a passive NGD network with an enhanced bandwidth based on asymmetrical directional coupler has been reported [10]. However, this structure requires optimization methods to get the coupling coefficients of multisection directional couplers.

In this article, a novel method to design a distributed transmission line NGD networks with enhanced bandwidth is presented. The bandwidth of the proposed network can be controlled by a coupling coefficient between open stub resonators.

2. PROPOSED STRUCTURE OF TERMINATION NETWORKS

Figure 1(a) shows the conventional structure of NGD networks, which do not have coupling between two open stub resonators [6]. Figure 1(b) shows the proposed structure of NGD networks, which consists of resistor-connected stubs with a characteristic impedance Z_2 and an electrical length θ_2, a coupled line with characteristic impedances Z_{0e} and Z_{0o} and electrical length θ_3, and through line with a characteristic impedance Z_1 and electrical length θ_1. As the proposed NGD structure is symmetrical with respect to the center through line, odd- and even-mode analyses can be applied to find the performance of proposed circuit.

Under the odd-mode excitation, the proposed NGD structure can be represented as the equivalent half circuit shown in Figure 2(a). The odd-mode input impedance is given as shown in (1).

$$Z_{\text{in\_odd}} = \frac{Z_1 \tan(\theta_1/2)(A + jRB)}{RB + j(Z_1 B \tan(\theta_1/2) - A)} \tag{1}$$

where

$$A = Z_2 Z_{0o} \cot\theta_3 - Z_2^2 \tan\theta_2 \tag{2a}$$

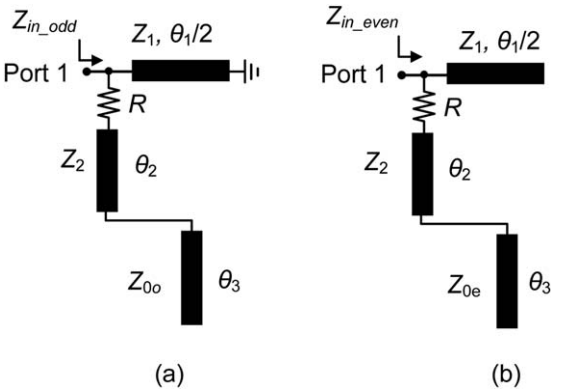

Figure 2 The equivalent half circuits under odd- and even-mode excitations: (a) odd-mode excitation and (b) even-mode excitation

$$B = Z_2 + Z_{0o}\cot\theta_3\tan\theta_2 \tag{2b}$$

Under the even-mode excitation, the proposed NGD network can be represented as the equivalent half circuit shown in Figure 2(b). The even-mode input impedance is given as shown in (3).

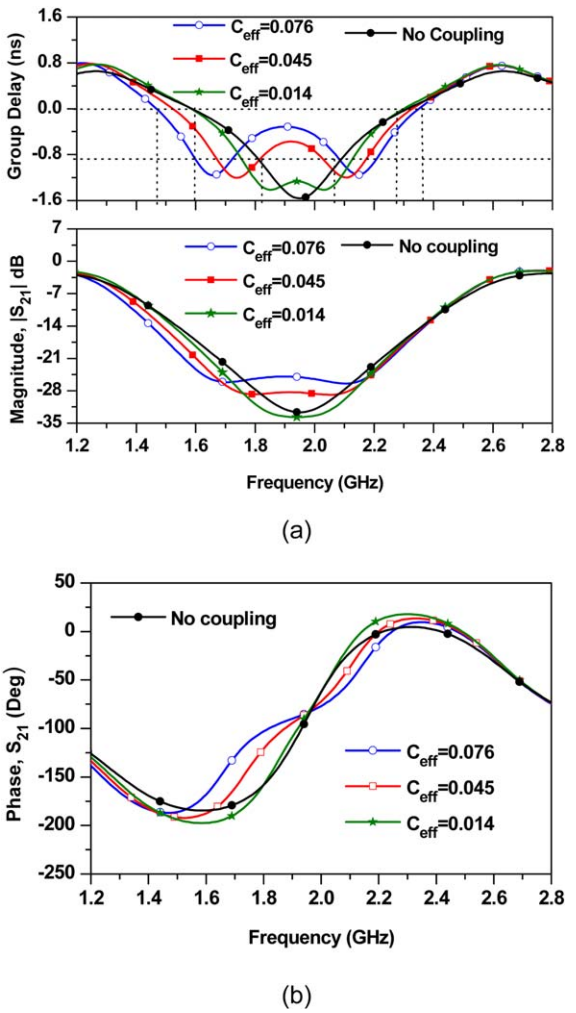

Figure 3 Simulated results of proposed NGD network: (a) GD/magnitude characteristics and (b) phase characteristics of S_{21}. [Color figure can be viewed in the online issue, which is available at wileyonlinelibrary.com]

$$Z_{\text{in\_even}} = \frac{Z_1\cot(\theta_1/2)(C - jRD)}{RD - j(Z_1 D\cot(\theta_1/2) - C)} \tag{3}$$

where

$$C = Z_2^2\tan\theta_2 - Z_2 Z_{0e}\cot\theta_3 \tag{4a}$$

$$D = Z_2 + Z_{0e}\cot\theta_3\tan\theta_2 \tag{4b}$$

Using these odd- and even-mode impedances [11], the S-parameters of the proposed circuit are given as shown in (5).

$$S_{11} = S_{22} = \frac{Z_{\text{in\_even}}Z_{\text{in\_odd}} - Z_0^2}{(Z_{\text{in\_even}} + Z_0)(Z_{\text{in\_odd}} + Z_0)} \tag{5a}$$

$$S_{21} = S_{12} = \frac{(Z_{\text{in\_even}} - Z_{\text{in\_odd}})Z_0}{(Z_{\text{in\_even}} + Z_0)(Z_{\text{in\_odd}} + Z_0)} \tag{5b}$$

where Z_0 is the port impedance. The group delay (GD) of the proposed circuit can be obtained using the following well-known relation.

$$\tau_g = -\frac{d\angle S_{21}}{d\omega} = -\frac{d}{d\omega}\left(\tan^{-1}\frac{\text{Im}(S_{21})}{\text{Re}(S_{21})}\right) \tag{5}$$

where $\text{Im}(S_{21})$ and $\text{Re}(S_{21})$ are the imaginary and real parts of the transmission coefficient (S_{21}), respectively. The coupling coefficient of the coupled line in the proposed circuit is defined as shown in (7).

$$C_{\text{eff}} = \frac{Z_{0e} - Z_{0o}}{Z_{0e} + Z_{0o}} \tag{6}$$

For the design graph, the GD, magnitude, and phase characteristics of the transmission coefficient (S_{21}) are plotted in Figure 3 for different values of C_{eff}. For this purpose, the circuit elements of the proposed circuit are assumed to be $Z_1 = Z_2 = 35$ Ω, $R = 3.5$ Ω, $\theta_1 = 90°$, and $\theta_2 = \theta_3 = 45°$ at the center frequency (f_0) for simplicity. The different values of C_{eff} according to the combination of Z_{0e} and Z_{0o} are given in Table 1. As seen in Figure 3(a), the NGD bandwidth can be enhanced by increasing C_{eff} of the coupled lines. As compared to the NGD network without coupling, the proposed network has two poles in the NGD time, which helps to enhance the NGD bandwidth. However, the flatness of NGD is degraded. Therefore, there is a trade-off between the NGD magnitude flatness, S_{21} magnitude flatness, and the NGD bandwidth. Figure 3(b) shows the phase characteristics of the proposed wideband NGD network under the different values of C_{eff}. As seen from this figure, the slope of S_{21} is positive over a wide frequency range, which signifies the presence of NGD over a wide bandwidth.

3. EXPERIMENTAL VERIFICATION

To verify the design method of the proposed structure, the NGD network with a GD of -1.2 ns operating at $f_0 = 1.96$ GHz was

TABLE 1 Odd- and Even-Mode Impedances of the Coupled Lines

Z_{0e} (Ω)	Z_{0o} (Ω)	C_{eff}
35	30	0.076
35	32	0.045
35	34	0.014
35	35	No coupling

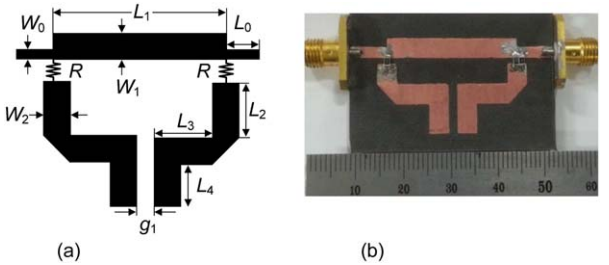

Figure 4 (a) EM simulation layout and (b) photograph of fabricated wideband NGD network. [Color figure can be viewed in the online issue, which is available at wileyonlinelibrary.com]

designed and fabricated. The EM simulation layout of the proposed network is shown in Figure 4(a). The circuit was fabricated on a Rogers RT/Duroid 5880 substrate with a dielectric constant (ε_r) of 2.2 and a thickness (h) of 31 mils. The EM simulation was performed using HFSS v15. The parameters of the fabricated circuit after the EM simulation are given as: $R = 3.5\ \Omega$, $W_0 = 2.4$, $L_0 = 5$, $W_1 = 4.20$, $L_1 = 28$, $W_2 = 4.2$, $L_2 = 4.4$, $L_3 = 11$, $L_4 = 6.30$, and $g_1 = 1.8$ (unit: millimeter). A photograph of the fabricated circuit is shown in Figure 4(b) and the overall circuit size is 40×35 mm^2.

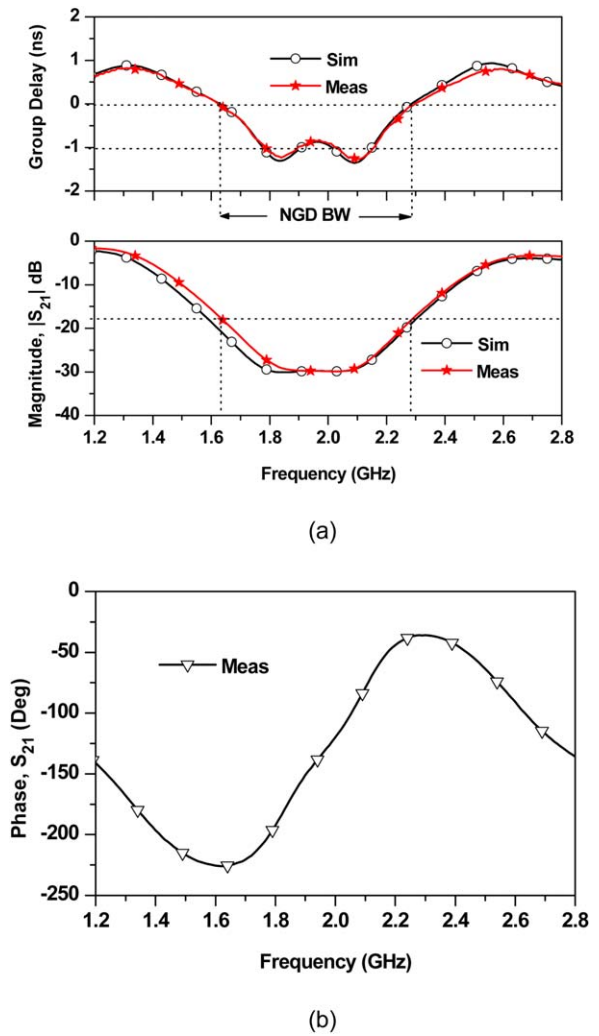

Figure 5 Simulation and measurement results: (a) GD/magnitude characteristics and (b) phase characteristics of S_{21}. [Color figure can be viewed in the online issue, which is available at wileyonlinelibrary.com]

Figure 5(a) shows the simulation and measurement results of the proposed NGD network. As seen in these figures, the measurement results are in good agreement with the simulation results. From the measurements, a maximum achievable NGD value of -1.1 ± 0.1 ns over the frequency range of 1.76−2.75 GHz was obtained, which shows the widest bandwidth as compared to previous works [2, 6, 7]. Therefore, NGD-bandwidth product of the proposed circuit is given as 0.451. The maximum signal attenuation (S_{21}) was found to be 29.30 dB at $f_0 = 1.96$ GHz. Figure 5(b) shows the measured phase characteristics of S_{21}, where the phase slope is positive over a certain frequency range which can be used for the wideband phase compensation.

4. CONCLUSION

In this article, the design of a compact wideband NGD network is presented. The NGD bandwidth can be controlled by the changing coupling coefficient between open stubs. For the experimental verification, the NGD network operating at a center frequency of 1.96 GHz was designed and fabricated. The measurement results were in good agreement with the simulations. The proposed network can provide a wideband NGD, is simple to design and is expected to be applicable for wideband communication systems.

ACKNOWLEDGMENT

This work was supported by the Basic Science Research Program through the National Research Foundation of Korea (NRF) funded by the Ministry of Education, Science and Technology (2013006660).

REFERENCES

1. M. Kitano, T. Nakanishi, and K. Sugiyama, Negative group delay and superluminal propagation: An electronic approach, IEEE J Sel Top Quantum Electron 9 (2003), 43–51.
2. L. Brillouin and A. Sommerfeld, Wave propagation and group velocity, 1960, pp. 113–137.
3. H. Choi, Y. Jeong, C.D. Kim, and J.S. Kenney, Efficiency enhancement of feedforward amplifiers by employing a negative group delay circuit, IEEE Trans Microwave Theory Tech 58 (2010), 1116–125.
4. B. Ravelo, M. L. Roy, and A. Perennec, Application of negative group delay active circuits to the design of broadband and constant phase shifters, Microwave Opt Tech Lett 50 (2008), 3078–3080.
5. S. Lucyszyn and I.D. Robertson, Analog reflection topology building blocks for adaptive microwave signal processing applications, IEEE Trans Microwave Theory Tech 43 (1995), 601–611.
6. G. Chaudhary and Y. Jeong, Microstrip line negative group delay filters for microwave circuits, IEEE Trans Microwave Theory Tech 62 (2014), 234–243.
7. B. Ravelo, A. Perennec, M.L. Roy, and Y.G. Boucher, Active microwave circuit with negative group delay, IEEE Microwave Wireless Compon Lett 17 (2007), 861–863.
8. H. Mirzaei and G.V. Eleftheriades, Realizing non-Foster reactive elements using negative group delay networks, IEEE Trans Microwave Theory Tech 61 (2013), 4322–4332.
9. O.F. Sidhiqui, M. Mojahedi, and G.V. Eleftheriades, Periodically loaded transmission line with effective negative group delay index and negative group velocity, IEEE Trans Antenna Propag 51 (2010), 2619–2625.
10. C.T. Michael, S. Gharavi, and T. Itoh, Negative group delay circuit based on a multisection asymmetrical directional coupler, In: Proceedings of IEEE Asia-pacific Microwave Conference, 2013.
11. J.S. Hong and M.J. Lancaster, Microstrip filters for RF/microwave applications, Wiley, New York, NY, 2001, pp. 19–21.